An all Mach number relaxation upwind scheme

Christophe Berthon *, Christian Klingenberg †, Markus Zenk ‡

June 12, 2018

Abstract

The present paper concerns the derivation of finite volume methods to approximate the weak solutions of the Euler equations within all Mach number regimes. To address such an issue, we develop a Suliciu relaxation type scheme. By adopting a relevant scaling according to the Mach number, the obtained numerical scheme is proved to be accurate in the sense that the numerical viscosity does not increase as soon as the Mach number tends to zero. Moreover, the obtained scheme is proved to be asymptotic preserving since the correct incompressible asymptotic regime is recovered in the limit of the Mach number to zero. In addition, the robustness of the method is established since both density and internal energy remain positive during the simulations. Several numerical experiments in 1D and 2D are performed to illustrate the relevance of the proposed low Mach number numerical scheme.

Keywords: Hyperbolic system; Euler flow; Low Mach number flows; asymptotic preserving schemes; relaxation schemes; upwind schemes

Subjectclass: [2000]65M60, 65M12

1 Introduction

In this work, we consider the approximation of the solutions of the compressible Euler equations of gas dynamics in 2 space dimensions. The system under consideration is given by

$$\begin{cases} \rho_t + (\rho u)_x + (\rho v)_y = 0, \\ (\rho u)_t + (\rho u^2 + p)_x + (\rho uv)_y = 0, \\ (\rho v)_t + (\rho vu)_x + (\rho v^2 + p)_y = 0, \\ E_t + (u(E+p))_x + (v(E+p))_y = 0, \end{cases} \tag{1}$$

*Laboratoire de Mathématiques Jean Leray, CNRS UMR 6629, Université de Nantes,2 rue de la Houssinière, BP 92208, 44322 Nantes, France.

†Universität Würzburg, Campus Hubland Nord, Emil-Fischer-Strasse 30, 97074 Würzburg, Germany.

‡Universität Würzburg, Campus Hubland Nord, Emil-Fischer-Strasse 30, 97074 Würzburg, Germany.

where $\rho(x,y,t) > 0$ denotes the density, $u(x,y,t)$ and $v(x,y,t)$ in $\mathbb{R}$ are the velocities and $E(x,y,t) > 0$ is the total energy. The pressure law $p(\rho,e) : \mathbb{R}^+ \times \mathbb{R}^+ \to \mathbb{R}^+$ is given by a general function such that

$$p\partial_e p + \rho^2 \partial_\rho p > 0,$$

in order to enforce the system (1) to be hyperbolic. The quantity $e(x,y,t) > 0$ stands for the internal energy such that

$$E = \rho e + \rho \frac{u^2 + v^2}{2}.$$

The characteristic nature of the flow is governed by dimensionless quantities like the Mach number M which controls the ratio of the velocity versus the sound speed. In this work, we consider solutions in regimes only governed by the Mach number M. Hence, we rewrite the system (1) in a non-dimentionalized form. Arguing standard rescaling (see [5], [18], [9]), we get the following set of equations where the Mach number M stands for a given parameter:

$$\begin{cases} \rho_t + (\rho u)_x + (\rho v)_y = 0, \\ (\rho u)_t + \left(\rho u^2 + \dfrac{p}{M^2}\right)_x + (\rho uv)_y = 0, \\ (\rho v)_t + (\rho vu)_x + \left(\rho v^2 + \dfrac{p}{M^2}\right)_y = 0, \\ E_t + (u(E+p))_x + (v(E+p))_y = 0, \end{cases} \tag{2}$$

with the following definition for the total energy:

$$E = \rho e + M^2 \rho \frac{u^2 + v^2}{2}. \tag{3}$$

To shorten notations, we introduce

$$w = \begin{pmatrix} \rho \\ \rho u \\ \rho v \\ E \end{pmatrix}, \qquad f(w) = \begin{pmatrix} \rho u \\ \rho u^2 + \frac{p}{M^2} \\ \rho uv \\ u(E+p) \end{pmatrix}, \qquad g(w) = \begin{pmatrix} \rho v \\ \rho uv \\ \rho v^2 + \frac{p}{M^2} \\ v(E+p) \end{pmatrix}, \tag{4}$$

so that the system (2) can be written in the following compact form:

$$w_t + f(w)_x + g(w)_y = 0. \tag{5}$$

The system (2)-(3) is associated with the following set of physical admissible states:

$$\Omega_M = \{w \in \mathbb{R}^4; \rho > 0, e > 0\}. \tag{6}$$

From now on, let us emphasize that the nature of the system (2)-(3) may drastically change depending to the values of M. Indeed, with large values of M, we have to deal with a hyperbolic system while the problem becomes elliptic

in the limit of M to zero. In the case of a barotropic model, i.e. the pressure law does not depend on the internal energy e, Klainermann and Majda [2] established that the compressible model tends to the incompressible counterpart given by

$$\begin{cases} u_t + uu_x + vu_y + \bar{p}_x = 0, \\ v_t + uv_x + vv_y + \bar{p}_y = 0, \\ u_x + v_y = 0, \\ \rho = const. \end{cases} \tag{7}$$

This is a remarkable result, since the limit pressure now satisfies the following elliptic equation:

$$\Delta \bar{p} = -(uu_x + vu_y)_x - (uv_x + vv_y)_x.$$

Next, considering the full Euler system (2)-(3), the limit behavior is proven in [24]. In the limit of M to 0, the incompressible model is recovered in a sense to be prescribed, and both kinetic and internal energies are proved to be thus conserved quantities.

In this work, we are interested to approximate solutions which are in the low Mach number regime, i.e. $M \ll 1$, as well as in the high Mach number regime. While standard upwind finite volume schemes produce good approximation with large value of M, it has been shown that they often lack in accuracy within the low Mach number regime (for instance, see [5, 8, 23]). More precisely, in the low Mach number regime, standard upwind schemes suffer from excessive numerical diffusion. For instance, the Roe scheme [20] introduces a diffusion which scales as $1/M$. As a consequence, the numerical viscosity dominates the approximate solution as soon as the Mach number is close to zero (see [8,18,30]). To cure such a failure, a wide range of preconditioners have been developed to modify the diffusion matrix of upwind schemes. In the present paper, we will also address this issue in our design of a low Mach number scheme.

To avoid these drastic numerical errors, several approaches have been developed to design low Mach number schemes. The first concept we want to mention is the so called asymptotic preserving schemes. In fact, the limit behavior depends on the parameter M. The numerical scheme in turn should be consistent with this limit behavior according to the governing parameter. In this case, a discretization for the compressible Euler equations should tend, in a prescribed sense, to a discretization of the incompressible Euler equations when M tends to zero (see Figure 1).

A distinct widely used approach to deal with this problem is to split the stiff and non-stiff terms in the system (2)-(3) and discretize them in different ways to ensure the stability of the scheme. This leads to the well-known IMEX approach (for example, see [6, 14, 16, 22, 25]). In general, the stiff part of system (2)-(3) is strongly related to the pressure term and therefore these splitting approaches often fall in the spirit of Klein [21]. Here, we also make use of this approach and a split of the pressure term into fast and slow fluctuations is proposed.

Finally, we want to emphasize on a particular analysis of the scaling of the dependent variables in the low Mach number regime (for instance, see [1, 5, 23]

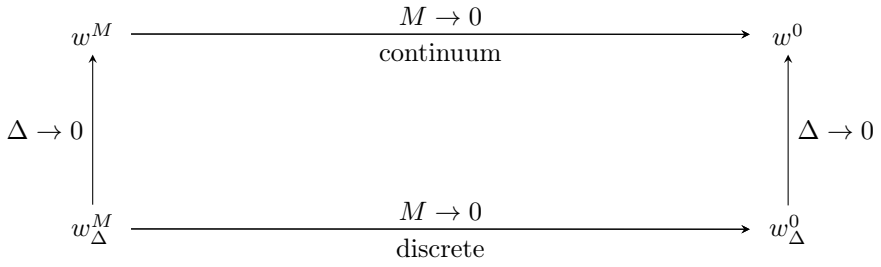

Figure 1: Asymptotic Preserving Diagram: w^M is a solution of system (2)-(3) and w^0 is a solution to (7) and w^M_Δ and w^0_Δ are discrete approximations to the respective solutions.

and references therein). These computations give a constraint on the scaling of the different variables with respect to the Mach number in order to achieve the incompressible limit equations. For the sake of clarity, we briefly review these computations.

Within the low Mach number regime, the unknowns can be rescaled according to M as follows:

$$\rho = \rho_0 + M\rho_1, \quad u = u_0 + Mu_1, \quad v = v_0 + Mv_1, \quad e = e_0 + Me_1, \tag{8}$$

where, to simplify the notations, we have omitted both space (x, y) and time t dependencies.

For instance, under open boundary assumptions, from (2)-(3), we deduce that the zero-order terms satisfy

$$\nabla\rho_0 = 0 \qquad \text{and} \qquad \nabla \cdot \begin{pmatrix} u_0 \\ v_0 \end{pmatrix} = 0, \tag{9}$$

while the pressure law must verify

$$p = p_0 + M^2 p_2 \qquad \text{and} \qquad \nabla p_0 = 0. \tag{10}$$

It is worth noticing that the space dependent zero-order velocities (u_0, v_0) satisfy the free divergence condition (9) but they satisfy

$$\partial_x u_0 = O(1) \quad \text{and} \quad \partial_y v_0 = O(1). \tag{11}$$

This remark will be essential in the sequel when studying the asymptotic behavior of numerical viscosity.

As strongly underlined in [1, 5, 23], standard upwind schemes generally violate the expected scaling of the pressure. For instance, the Roe scheme [20] introduces pressure fluctuations of order $O(M)$ and therefore the incompressible limit might not be achieved as well as this leads to excessive numerical diffusion.

According to (9) and (10), we define a set of asymptotic preserving states as follows:

$$\Omega_0 = \left\{ w_0 \in \mathbb{R}^4; \nabla\rho_0 = 0, \nabla p_0 = 0, \nabla \cdot \begin{pmatrix} u_0 \\ v_0 \end{pmatrix} = 0 \right\}. \tag{12}$$

In order to produce physical relevant results, we naturally demand that Ω_0 is an invariant region for the designed upwind scheme. Moreover, we can strengthen the definition of the invariant region by combining (6) and (12) to get

$$\Omega = \Omega_M \cap \Omega_0, \tag{13}$$

and by imposing Ω to be an invariant region. In other words, we enforce the derived relaxation up-wind scheme to preserve Ω, to control the numerical diffusion according to the Mach number fluctuations, and to recover the correct asymptotic incompressible regime.

The present work is structured as follows. In Section 2, for the sake of completeness, we recall the numerical framework of the Godunov-type scheme [12]. Next, we design a Suliciu relaxation model according to the usual approach [3, 4, 13, 27]. Unfortunately, the usual approach does not yield to the required numerical viscosity as soon as the Mach number is small enough. To correct such a failure, in Section 3,we introduce a suitable Suliciu relaxation model where fast and slow phenomenon are relevantly split. The scheme obtained thus is proved to satisfy the required properties in the limit of the Mach number to zero. Finally, in section 4 we give numerical results to show the applicability of the scheme.

2 Numerical Scheme

Since the Euler system (2)-(3) under consideration is known to be invariant by Galilean rotations, we here describe the discretization of the associated 1D model given by

$$w_t + f(w)_x = 0, \tag{14}$$

where w and $f(w)$ are defined by (4). Let us underline that the 2D extension turns out to be obvious (for instance, see [11, 19]).

In the present work, we adopt a finite volume scheme of Godunov-type [12]. To address such an issue, the space is discretized by considering an uniform mesh made of cells $(x_{i-\frac{1}{2}}, x_{i+\frac{1}{2}})$ of constant size Δx. In addition, we adopt a constant time step Δt such that $t^n = n\Delta t$.

At time t^n, we define the following piecewise constant function:

$$w^n(x, t^n) = w_i^n, \quad x \in (x_{i-\frac{1}{2}}, x_{i+\frac{1}{2}}) \quad \text{for all } i \in \mathbb{Z},$$

to be an approximation of the solution of (14). Next, this approximation is evolved to get an updated approximation at time $t^n + \Delta t$. According to the pioneer work by Harten, Lax and van Leer [12], we introduce $\tilde{w}_{\mathcal{R}}(x/t; w_L, w_R)$

an approximate Riemann solver in the form

$$\tilde{w}_{\mathcal{R}}\left(\frac{x}{t};w_L,w_R\right)=\begin{cases} w_L \quad \text{if } \dfrac{x}{t}<\lambda_L(w_L,w_R),\\ w^{\star}\left(\dfrac{x}{t};w_L,w_R\right) \quad \text{if } \lambda_L(w_L,w_R)<\dfrac{x}{t}<\lambda_R(w_L,w_R),\\ w_R \quad \text{if } \dfrac{x}{t}>\lambda_R(w_L,w_R), \end{cases} \tag{15}$$

which satisfies the following integral consistency condition:

$$\frac{1}{\Delta x}\int_{-\frac{\Delta x}{2}}^{\frac{\Delta x}{2}}\tilde{w}_{\mathcal{R}}\left(\frac{x}{\Delta t};w_L,w_R\right)dx=\frac{1}{2}(w_L+w_R)-\frac{\Delta t}{\Delta x}(f(w_R)-f(w_L)). \tag{16}$$

Equipped with this approximate Riemann solver, we evolve $w^n(x,t^n+t)$ in time as follows:

$$\begin{aligned} w^n(x,t^n+t)=&\tilde{w}_{\mathcal{R}}\left(\frac{x-x_{i+\frac{1}{2}}}{t};w_i^n,w_{i+1}^n\right),\\ &x\in\left(x_{i+\frac{1}{2}}-\frac{\Delta x}{2},x_{i+\frac{1}{2}}+\frac{\Delta x}{2}\right) \quad \text{for all } i\in\mathbb{Z}. \end{aligned}$$

From now on, let us emphasize that this time evolution is nothing but the juxtaposition of the approximate Riemann solvers stated at each interface $x_{i+\frac{1}{2}}$ for all i in $\mathbb{Z}$. In order to avoid interactions between all the approximate Riemann solvers, we impose the following CFL-like condition:

$$\frac{\Delta t}{\Delta x}\max_{i\in\mathbb{Z}}\left(|\lambda_L(w_i^n,w_{i+1}^n)|,|\lambda_R(w_i^n,w_{i+1}^n)|\right)\leq\frac{1}{2}.$$

Furthermore, let us underline that the functions λ_L and λ_R may depend on the Mach number M and such a CFL condition may become very restrictive as soon as M goes to zero. As a consequence, an implicit time discretization will be adopted to perform numerical simulations. However, the forthcoming numerical developments do not depend on whether explicit or implicit formulations are used.

Now, we are able to give the updated states at time t^{n+1}as follows:

$$w_i^{n+1}=\frac{1}{\Delta x}\int_{x_{i-\frac{1}{2}}}^{x_{i+\frac{1}{2}}}w^n(x,t^n+\Delta t)dx.$$

According to the integral consistency condition (16), the updated states rewrite

$$w_i^{n+1}=w_i^n-\frac{\Delta t}{\Delta x}\left(f(w_i^n,w_{i+1}^n)-f(w_{i-1}^n,w_i^n)\right), \tag{17}$$

where the numerical flux function reads

$$\begin{aligned} f(w_L,w_R)&=f(w_L)+\frac{\Delta x}{2\Delta t}w_L-\frac{1}{\Delta t}\int_{-\frac{\Delta x}{2}}^{0}\tilde{w}_{\mathcal{R}}\left(\frac{x}{\Delta t};w_L,w_R\right)dx,\\ &=f(w_R)-\frac{\Delta x}{2\Delta t}w_R+\frac{1}{\Delta t}\int_{0}^{\frac{\Delta x}{2}}\tilde{w}_{\mathcal{R}}\left(\frac{x}{\Delta t};w_L,w_R\right)dx. \end{aligned} \tag{18}$$

Now, the main objective is to derive a relevant approximate Riemann solver $\tilde{w}_{\mathcal{R}}$. To access such an issue, we suggest to consider the usual Suliciu relaxation approach [3,10,10,13,27] where the nonlinear pressure p is substituted by a new variable π. This new variable π is governed by the following equation:

$$\pi_t + u\pi_x + \frac{c^2}{\rho} u_x = \frac{1}{\epsilon}(p - \pi). \tag{19}$$

The relaxation parameter c is fixed according to some stability and robustness properties. As a consequence, the Suliciu relaxation model now reads

$$\begin{cases} \rho_t + (\rho u)_x = 0, \\ (\rho u)_t + \left(\rho u^2 + \dfrac{\pi}{M^2}\right)_x = 0, \\ (\rho v)_t + (\rho u v)_x = 0, \\ E_t + (u(E+\pi))_x = 0, \\ (\rho\pi)_t + (\rho u \pi + c^2 u)_x = \dfrac{\rho}{\epsilon}(p - \pi). \end{cases} \tag{20}$$

Let us notice that, in the limit of ϵ to zero, formally the relaxation source term implies that π converges to the expected pressure law p and then the sub-system extracted from (20) to govern w coincides with the expected Euler model (14).

For the sake of simplicity in the notations, let us set

$$U = {}^t(\rho, \rho u, \rho v, E, \rho\pi).$$

Moreover, let us note $(20)_{\varepsilon=\infty}$ the homogeneous system extracted from (20). Now, we are interested in the derivation of the Riemann solution associated with $(20)_{\varepsilon=\infty}$. First, in the following result, we give the nature of each field. The proof of this result is standard (for instance, see [11]) and it is omitted here.

Lemma 1. *The homogeneous system extracted from (20) is hyperbolic with eigenvalues $\lambda_\pm = u \pm \frac{\rho}{cM}$ and $\lambda_c = u$, where λ_c has multiplicity three. All the fields are linearly degenerated.*

Now, we consider an initial data given by

$$U(x, t=0) = \begin{cases} U_L & \text{if } x < 0, \\ U_R & \text{if } x > 0. \end{cases} \tag{21}$$

According to Lemma 1, the Riemann solution of $(20)_{\varepsilon=\infty}$ consists of piecewise constant states separated by contact discontinuities in the following form:

$$U_{\mathcal{R}}\left(\frac{x}{t}; U_L, U_R\right) = \begin{cases} U_L & \text{if } \frac{x}{t} < \lambda_-, \\ U_L^* & \text{if } \lambda_- < \frac{x}{t} < \lambda_c, \\ U_R^* & \text{if } \lambda_c < \frac{x}{t} < \lambda_+, \\ U_R & \text{if } \frac{x}{t} > \lambda_+, \end{cases} \tag{22}$$

where the intermediate states are given by (see [7, 10])

$$
\begin{aligned}
&\pi_C = \pi_L^* = \pi_R^* = \frac{\pi_L + \pi_R}{2} - cM\frac{u_R - u_L}{2},\\
&u_C = u_L^* = u_R^* = \frac{u_L + u_R}{2} - \frac{\pi_R - \pi_L}{2cM},\\
&\rho_L^* = \frac{1}{\frac{1}{\rho_L} + \frac{\pi_C - \pi_L}{c^2}}, \qquad \rho_R^* = \frac{1}{\frac{1}{\rho_R} + \frac{\pi_R - \pi_C}{c^2}},\\
&e_L^* = e_L - \frac{\pi_L^2 - \pi_C^2}{2c^2}, \qquad e_R^* = e_R - \frac{\pi_R^2 - \pi_C^2}{2c^2},\\
&v_L^* = v_L, \qquad v_R^* = v_R,
\end{aligned}
\tag{23}
$$

with the internal energy e defined by (3).

From (22) and (23), we now give the Suliciu relaxation approximate Riemann solver needed to fully define the scheme (17)-(18). Let us introduce

$$
\begin{aligned}
&U^{eq}(w) = {}^t(\rho, \rho u, \rho v, E, \rho p(\rho, e)),\\
&QU = {}^t(\rho, \rho u, \rho v, E),
\end{aligned}
$$

to define the required approximate Riemann solver as follows:

$$
\tilde{w}_{\mathcal{R}}\left(\frac{x}{\Delta t}; w_L, w_R\right) = QU_{\mathcal{R}}\left(\frac{x}{t}; U^{eq}(w_L), U^{eq}(w_R)\right). \tag{24}
$$

In order to exhibit the behavior of the numerical diffusion within the asymptotic regime in the limit of M to zero, we enforce the Mach number rescaling given in (8). We consider $w_0 \in \Omega_0$ to write

$$
w_L = w_{0,L} + O(M) \quad \text{and} \quad w_R = w_{0,R} + O(M).
$$

Next, since $\nabla\rho_0 = 0$ from (9), with no restriction we can assume that $\rho_{0,L} = \rho_{0,R} = \rho_0$. Similarly, from (10), we have $\nabla p_0 = 0$ and then we can assume $p_{0,L} = p_{0,R} = p_0$ and $e_{0,L} = e_{0,R} = e_0$. As a consequence, we have

$$
\begin{aligned}
&\rho_L = \rho_0 + O(M), && \rho_R = \rho_0 + O(M),\\
&u_L = u_{0,L} + O(M), && u_R = u_{0,R} + O(M),\\
&v_L = v_{0,L} + O(M), && v_R = v_{0,R} + O(M),\\
&e_L = e_0 + O(M), && e_R = e_0 + O(M),\\
&\pi_L = p_0 + O(M^2), && \pi_R = p_0 + O(M^2).
\end{aligned}
\tag{25}
$$

Because of (11), it is worth noticing that

$$
u_{0,R} - u_{0,L} = O(1). \tag{26}
$$

These expressions are now adopted to exhibit the behavior of the intermediate states U_L^* and U_R^*. First, let us focus on the intermediate pressure π_C defined by (23). According to (25), we obtain

$$
\pi_C = \left(p_0 + O(M^2)\right) - \frac{cM}{2}\left(u_{0,R} - u_{0,L} + O(M)\right). \tag{27}
$$

Arguing (26), we easily have

$$\pi_C = p_0 + O(M). \tag{28}$$

We immediately notice that the intermediate pressure π_C admits variations of the order $O(M)$ instead of variations of the order $O(M^2)$.

Concerning the other quantities, once again from (23) and (25), we get

$$\begin{cases} u_C = \dfrac{u_{0,L} + u_{0,R}}{2} + O(M), & \\ v_L^* = v_{0,L} + O(M), & v_R^* = v_{0,R} + O(M), \\ \rho_L^* = \rho_0 + O(M), & \rho_R^* = \rho_0 + O(M), \\ e_L^* = e_0 + O(M), & e_R^* = e_0 + O(M). \end{cases} \tag{29}$$

Equipped with the behavior of the approximate Riemann solver, we are now able to exhibit the numerical viscosity. Let us remark that the numerical flux function rewrites

$$f(w_L, w_R) = \frac{1}{2}(f(w_L) + f(w_R)) - \frac{1}{2}D(w_R - w_L),$$

where D stands for the sought numerical diffusion matrix. Using the scaling (29), (28) and (29), and plugging them into both exact and numerical flux functions, we obtain

$$\begin{aligned} D(w_R - w_L) &= \frac{1}{2}(f(w_L) + f(w_R)) - f(w_L, w_R), \qquad (30) \\ &= \begin{pmatrix} \rho_0 u_{0,L/R} + O(1) \\ \rho_0 u_{0,L/R}^2 + \frac{p_0}{M^2} + O(1) \\ \rho_0 u_{0,L/R} v_{0,L/R} + O(1) \\ u_{0,L/R}(E_0 + p_0) + O(1) \end{pmatrix} - \begin{pmatrix} \rho_0 u_{0,L/R} + O(1) \\ \rho_0 u_{0,L/R}^2 + \frac{p_0}{M^2} + O(\frac{1}{M}) \\ \rho_0 u_{0,L/R} v_{0,L/R} + O(1) \\ u_{0,L/R}(E_0 + p_0) + O(1) \end{pmatrix}, \\ &= \begin{pmatrix} O(1) \\ O(\frac{1}{M}) \\ O(1) \\ O(1) \end{pmatrix} \qquad (31) \end{aligned}$$

Therefore we can expect excessive diffusion in the momentum orthogonal to the interface in the low Mach number regime. As a consequence, the standard Suliciu relaxation scheme turns out to be non-relevant to approximate solutions in the low Mach number regime.

At this level, let us underline that the main failure in deriving the Suliciu relaxation solver stays in (26). Indeed, as soon as $u_{0,R} - u_{0,L} = O(M)$, we immediately recover the required behavior of the diffusion matrix. Such a good situation is satisfied for fully 1D simulations. Of course, we are here considering 2D problems and, unfortunately, the condition (26) holds true.

We have thus seen that the standard version of the Suliciu relaxation is not suited for approximating low Mach number flows in more then one space dimension. However, we also conclude, that the main problem is in the scaling

of the intermediate relaxation pressure π_C. Since this relaxation technique relies on controlling a relaxation pressure, it seems natural to search for a different control of the relaxation pressure in order to achieve the asymptotic behavior of the intermediate states. This is the purpose of the next section.

3 All Mach number Relaxation Model

To cure the deficiencies of the model presented in section 2, we now propose a different relaxation model capable to accurately capture low Mach number flows. We follow the spirit of Klein et al. [28] by adopting a splitting of the pressure into a slow dynamics pressure and a fast acoustics pressure.

We suggest to decompose the scaled pressure as follows:

$$\frac{p}{M^2} = \frac{M_{loc}^2}{M^2} p + \frac{1 - M_{loc}^2}{M^2} p, \tag{32}$$

where $M_{loc} \in [0, 1]$ denotes a given parameter. From a practical point of view, M_{loc} will be defined as a local Mach number derived from local flow properties. Of course, with $M \leq 1$, $M_{loc} = M$ is a relevant choice but, according to numerical simulations of interest, it is more convenient to consider M_{loc} as a free parameter.

In (32), the quantity $\frac{M_{loc}^2}{M^2} p$ corresponds to the slow dynamics pressure while $\frac{1-M_{loc}^2}{M^2} p$ stands for the fast acoustics pressure. Now, in the spirit of the standard Suliciu relaxation approach, we substitute both slow and fast pressures by new unknowns. We thus introduce $\frac{M_{loc}^2}{M^2}\pi$ and $\frac{1-M_{loc}^2}{M^2}\psi$, the new variables, to respectively represent the slow and fast pressures. As a consequence, the momentum equation in (14) is here substituted by

$$(\rho u)_t + \left(\rho u^2 + \frac{M_{loc}^2}{M^2}\pi + \frac{1 - M_{loc}^2}{M^2}\psi \right)_x = 0.$$

Next, evolution laws satisfied by the new unknowns π and ψ must be proposed. Since the usual Suliciu relaxation model is relevant for slow dynamics pressure, we adopt the equation (19) to govern π. In fact, the situation turns out to be more delicate to evolve the unknown ψ. Indeed, adopting (19) to evolve ψ yields to non-relevant diffusion terms in the full numerical scheme. To correct such a failure, we adopt the following evolution law:

$$\psi_t + u\psi_x + \frac{c^2}{\rho}\bar{u}_x = \frac{1}{\epsilon}(p - \psi), \tag{33}$$

where $\bar{u}$ coincides with a relaxed velocity governed as follows:

$$\bar{u}_t + u\bar{u}_x + \frac{1}{\rho M_{loc}^2 M^2}\psi_x = \frac{1}{\epsilon}(u - \bar{u}). \tag{34}$$

We are now able to give the all Mach number Suliciu relaxation model of interest in the present work

$$\begin{cases} \rho_t + (\rho u)_x = 0, \\ (\rho u)_t + \left(\rho u^2 + \dfrac{M_{loc}^2}{M^2}\pi + \dfrac{1 - M_{loc}^2}{M^2}\psi \right)_x = 0, \\ (\rho v)_t + (\rho v u)_x = 0, \\ E_t + (u(E + M_{loc}^2\pi + (1 - M_{loc}^2)\psi)_x = 0, \\ (\rho\pi)_t + (\rho u\pi + c^2 u)_x = \dfrac{\rho}{\epsilon}(p - \pi), \\ (\rho\psi)_t + (\rho u\psi + c^2\bar{u})_x = \dfrac{\rho}{\epsilon}(p - \psi), \\ (\rho\bar{u})_t + \left(\rho u\bar{u} + \dfrac{1}{M_{loc}^2 M^2}\psi \right)_x = \dfrac{\rho}{\epsilon}(u - \bar{u}). \end{cases} \tag{35}$$

Once again, let us emphasize that in the limit of ϵ to zero, the relaxed unknowns π, ψ and $\bar{u}$ respectively converges, at least formally, to p, p and u. As a consequence, the evolution laws for $(\rho, \rho u, \rho v, E)$ in (35) coincide to the initial system (14).

To simplify the notation in the sequel, we set

$$W = {}^t(\rho, \rho u, \rho v, E, \rho\pi, \rho\psi, \rho\bar{u}) \qquad \text{and} \qquad W^{eq}(w) = {}^t(\rho, \rho u, \rho v, E, \rho p, \rho p, \rho u). \tag{36}$$

3.1 Stability of the relaxation system

After Whitham [31] (see also [4, 19, 29]), both equilibrium system (14) and relaxation model (35) have to satisfy some compatibility conditions to prevent instabilities in the limit of ϵ to zero. These compatibility conditions are the so-called subcharacteristic conditions [31] to be put on the relaxation parameter c. In order to exhibit these restriction on c, several approaches have been proposed in the literature (for instance, see [4, 19, 29]). In the present work, we study the viscous asymptotic equilibrium system, in the limit of ϵ to zero, coming from a formal Chapman-Enskog expansion. To address such an issue, let us consider a small perturbation W^ϵ of a local equilibrium $w \in \Omega_M$ such that

$$\begin{aligned} \pi^\epsilon &= p(\rho, e) + \epsilon\pi^1 + O(\epsilon^2), \\ \psi^\epsilon &= p(\rho, e) + \epsilon\psi^1 + O(\epsilon^2), \\ \bar{u}^\epsilon &= u + \epsilon u^1 + O(\epsilon^2). \end{aligned} \tag{37}$$

By substituting (37) into (35) and neglecting higher order terms in ϵ, we get the following viscous equilibrium system (see Theorem 2):

$$w_t + f(w)_x = \epsilon(\mathcal{D}(w)w_x)_x, \tag{38}$$

where the flux function f is defined by (4) and $\mathcal{D}$ is a diffusion matrix.

Here, the stability requirement is obtained imposing the eigenvalues of $\mathcal{D}$ to be non-negative. In the next statement, we establish that such stability condition is verified as long as a subcharacteristic condition holds.

Theorem 2. *Assume that the relaxation parameter c satisfies the following subcharacteristic condition:*

$$c^2 > \rho^2 \partial_\rho p(\rho, e). \tag{39}$$

Then, the diffusion matrix in (38) has non-negative eigenvalues. As a consequence, the relaxation system (35) is a stable diffusive approximation of system (2)-(3).

Proof. Adopting the Chapman-Enskog expansion (37), we evaluate the first-order correctors π^1, ψ^1 and $\bar{u}^1$. First, from (35), we immediately get

$$\begin{aligned}
\pi^\epsilon &= p - \epsilon \left(\pi_t^\epsilon + u \pi_x^\epsilon + \frac{c^2}{\rho} u_x \right), \\
\psi^\epsilon &= p - \epsilon \left(\psi_t^\epsilon + u \psi_x^\epsilon + \frac{c^2}{\rho} u_x \right), \\
\bar{u}^\epsilon &= u - \epsilon \left(\bar{u}_t^\epsilon + u \bar{u}_x^\epsilon + \frac{1}{\rho M_{loc}^2 M^2} \psi_x^\epsilon \right).
\end{aligned}$$

Substituting the expansions (37) into the above three relations, we obtain

$$\begin{aligned}
\pi^\epsilon &= p - \epsilon \left(p_t + u p_x + \frac{c^2}{\rho} u_x \right) + O(\epsilon^2), \\
\psi^\epsilon &= p - \epsilon \left(p_t + u p_x + \frac{c^2}{\rho} u_x \right) + O(\epsilon^2), \\
\bar{u}^\epsilon &= u - \epsilon \left(u_t + u u_x + \frac{c^2}{\rho M_{loc}^2 M^2} p_x \right) + O(\epsilon^2).
\end{aligned} \tag{40}$$

Next, from both conservation of mass and momentum in (35), a formal computation gives

$$\begin{aligned}
p_t + u p_x &= -\rho \partial_\rho p u_x \\
u_t + u u_x &= -\frac{p_x}{\rho M^2}
\end{aligned}$$

Let us plug these relations into (40) to write

$$\begin{aligned}
\pi^1 &= -\left(\frac{c^2}{\rho} - \rho \partial_\rho p \right) u_x + O(\epsilon), \\
\psi^1 &= -\left(\frac{c^2}{\rho} - \rho \partial_\rho p \right) u_x + O(\epsilon), \\
\bar{u}^1 &= -\left(\frac{1}{M_{loc}^2} - 1 \right) \frac{1}{\rho M^2} p_x + O(\epsilon).
\end{aligned}$$

Equipped with these first-order correctors, both momentum and energy equations now read

$$(\rho u)_t + \left(\rho u^2 + \frac{p}{M^2}\right)_x = \epsilon \left(\frac{1}{\rho M^2}(c^2 - \rho^2 \partial_\rho p) u_x\right)_x + O(\epsilon^2),$$
$$E_t + (u(E+p))_x = \epsilon \left(\frac{1}{\rho}(c^2 - \rho^2 \partial_\rho p)(\frac{u^2}{2})_x\right)_x + O(\epsilon^2).$$

By neglecting higher order terms in ϵ, we recover the viscous system (38) for a diffusion matrix given by

$$\mathcal{D} = \begin{pmatrix} 0 & 0 & 0 & 0 \\ -\frac{u}{\rho^2 M}(c^2 - \rho^2 \partial_\rho p) & \frac{1}{\rho^2 M}(c^2 - \rho^2 \partial_\rho p) & 0 & 0 \\ 0 & 0 & 0 & 0 \\ -\frac{u^2}{\rho^2}(c^2 - \rho^2 \partial_\rho p) & \frac{u}{\rho^2 M}(c^2 - \rho^2 \partial_\rho p) & 0 & 0 \end{pmatrix}.$$

The eigenvalues of $\mathcal{D}$ easily read 0 and $\frac{1}{\rho^2 M}(c^2 - \rho^2 \partial_\rho p)$ and therefore the diffusion matrix admits non-negative eigenvalues as long as the subcharacteristic condition (39) holds. The proof is thus achieved. □

3.2 Properties of the primitive relaxation system

In order to complete the definition of the numerical scheme (17)-(18),we have to exhibit the Riemann solution coming from the first-order homogeneous extracted system associated to the relaxation model (35). In the sequel, we denote $(35)_{\varepsilon=\infty}$ this first-order extracted system obtained in the limit of ε to infinity.

In the next statement, we give the expected Riemann solution. Next, this solution is studied and conditions are stated in order to enforce such solutions to belong to Ω_M. In a last result, we consider the particular case of M_{loc} close to 1.

Lemma 3. *The first-order homogeneous system extracted from(35) is hyperbolic and fully linear degenerate with eigenvalues*

$$\lambda_{s\pm}(W) = u \pm \frac{cM_{loc}}{\rho M}, \quad \lambda_{f\pm}(W) = u \pm \frac{c}{\rho M_{loc} M} \quad \textit{and} \quad \lambda_c(W) = u, \qquad (41)$$

where λ_c has multiplicity 3. Moreover, the solution to the Riemann problem is composed of 7 constant states separated by 5 contact discontinuities (see figure 2 as follows

$$W_{\mathcal{R}}(\frac{x}{t}; W_L, W_R) = \begin{cases} W_L \ \ if \ \frac{x}{t} < \lambda_{f-}(W), \\ W_{L^*} \ \ if \ \lambda_{f-}(W) < \frac{x}{t} < \lambda_{s-}(W), \\ W_{C^L} \ \ if \ \lambda_{s-}(W) < \frac{x}{t} < \lambda_c(W), \\ W_{C^R} \ \ if \ \lambda_c(W) < \frac{x}{t} < \lambda_{s+}(W), \\ W_{R^*} \ \ if \ \lambda_{s+}(W) < \frac{x}{t} < \lambda_{f+}(W), \\ W_R \ \ if \ \frac{x}{t} > \lambda_{f+}(W), \end{cases} \qquad (42)$$

where the intermediate states are given by

$$
\begin{aligned}
&\psi_{L^*} = \psi_{R^*} = \psi_{C^L} = \psi_{C^R} = \psi_C = \frac{\psi_L + \psi_R}{2} + cM_{loc}M\frac{\bar{u}_L - \bar{u}_R}{2},\\
&\bar{u}_{L^*} = \bar{u}_{R^*} = \bar{u}_{C^L} = \bar{u}_{C^R} = \bar{u}_C = \frac{\bar{u}_L + \bar{u}_R}{2} + \frac{\psi_L - \psi_R}{2cM_{loc}M},\\
&\pi_{C^L} = \pi_{C^R} = \pi_C = \frac{\pi_{L^*} + \pi_{R^*}}{2} + \frac{cM}{M_{loc}}\frac{(u_{L^*} - u_{R^*})}{2},\\
&u_{C^L} = u_{C^R} = u_C = \frac{u_{L^*} + u_{R^*}}{2} + \frac{M_{loc}}{cM}\frac{\pi_{L^*} - \pi_{R^*}}{2},\\
&e_{L^*} = e_L - \frac{M_{loc}^2}{2c^2}(\pi_L^2 - \pi_{L^*}^2 + \frac{1 - M_{loc}^2}{1 + M_{loc}^2}(\psi_L^2 - \psi_C^2)),\\
&e_{R^*} = e_R - \frac{M_{loc}^2}{2c^2}(\pi_R^2 - \pi_{R^*}^2 + \frac{1 - M_{loc}^2}{1 + M_{loc}^2}(\psi_R^2 - \psi_C^2)),\\
&e_{C^L} = e_{L^*} - \pi_{L^*}\frac{M_{loc}^2\pi_{L^*} + 2(1 - M_{loc}^2)\psi_C}{2c^2} + \pi_C\frac{M_{loc}^2\pi_C + 2(1 - M_{loc}^2)\psi_C}{2c^2},\\
&e_{C^R} = e_{R^*} - \pi_{R^*}\frac{M_{loc}^2\pi_{R^*} + 2(1 - M_{loc}^2)\psi_C}{2c^2} + \pi_C\frac{M_{loc}^2\pi_C + 2(1 - M_{loc}^2)\psi_C}{2c^2},\\
&\pi_{L^*} = \pi_L + \frac{M_{loc}^2}{1 + M_{loc}^2}(\psi_C - \psi_L), \qquad \pi_{R^*} = \pi_R + \frac{M_{loc}^2}{1 + M_{loc}^2}(\psi_C - \psi_R),\\
&u_{L^*} = u_L - \frac{M_{loc}}{cM^2(1 + M_{loc}^2)}(\psi_C - \psi_L), \quad u_{R^*} = u_R + \frac{M_{loc}}{cM^2(1 + M_{loc}^2)}(\psi_C - \psi_R),\\
&\rho_{L^*} = \frac{1}{\frac{1}{\rho_L} + \frac{\pi_L - \pi_{L^*}}{c^2}}, \qquad \rho_{R^*} = \frac{1}{\frac{1}{\rho_R} + \frac{\pi_R - \pi_{R^*}}{c^2}},\\
&\rho_{C^L} = \frac{1}{\frac{1}{\rho_L} + \frac{\pi_L - \pi_C}{c^2}}, \qquad \rho_{C^R} = \frac{1}{\frac{1}{\rho_R} + \frac{\pi_R - \pi_C}{c^2}},\\
&v_{L^*} = v_{C^L} = v_L, \qquad v_{R^*} = v_{C^R} = v_R.
\end{aligned}
\tag{43}
$$

From now on, let us underline that we have enforced the eigenvalues to be ordered in (42). Such an order will be justified in the next result devoted to the admissibility of the Riemann solutions.

In addition, from $W_{\mathcal{R}}$defined by (42)-(43), we are now able to give the all Mach number relaxation scheme according to (17)-(18). Let us introduce

$$
\begin{aligned}
&W^{eq}(w) = {}^t(\rho, \rho u, \rho v, E, \rho p(\rho, e), \rho p(\rho, e), \rho u),\\
&QW = {}^t(\rho, \rho u, \rho v, E).
\end{aligned}
$$

Then, the approximate Riemann solver introduced in (17)-(18) is defined as follows:

$$
\tilde{w}_{\mathcal{R}}\left(\frac{x}{\Delta t}; w_L, w_R\right) = QW_{\mathcal{R}}\left(\frac{x}{t}; W^{eq}(w_L), W^{eq}(w_R)\right). \tag{44}
$$

Now, we turn establishing Lemma 3.

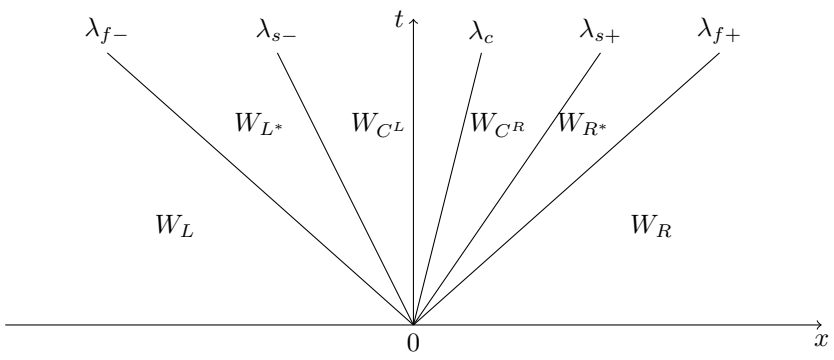

Figure 2: Wave structure of the Riemann problem

Proof. In order to exhibit the algebra of the first-order extracted system $(35)_{\varepsilon=\infty}$, it turns out to be convenient to consider the primitive variables given by

$$V = {}^t(\rho, u, v, e, \pi, \psi, \bar{u}),$$

where the internal energy e is defined by (3). Then, V is solution of the system

$$V_t + A(V)V_x = 0, \tag{45}$$

where the matrix $A(V)$ is given by

$$A(V) = \begin{pmatrix} u & \rho & 0 & 0 & 0 & 0 & 0 \\ 0 & u & 0 & 0 & \dfrac{M_{loc}^2}{\rho M^2} & \dfrac{1-M_{loc}^2}{\rho M^2} & 0 \\ 0 & 0 & u & 0 & 0 & 0 & 0 \\ 0 & \dfrac{M_{loc}^2\pi + (1-M_{loc}^2)\psi}{\rho} & 0 & u & 0 & 0 & 0 \\ 0 & \dfrac{c^2}{\rho} & 0 & 0 & u & 0 & 0 \\ 0 & 0 & 0 & 0 & 0 & u & \dfrac{c^2}{\rho} \\ 0 & 0 & 0 & 0 & 0 & \dfrac{1}{\rho M^2 M_{loc}^2} & u \end{pmatrix}$$

From direct computations, we easily obtain the eigenvalues of $A(V)$ given by (41) with the associated eigenvectors given as follows:

- with λ_c, the eigenvectors are $r_c^1 = \begin{pmatrix} 1 \\ 0 \\ 0 \\ 0 \\ 0 \\ 0 \\ 0 \end{pmatrix}$, $r_c^2 = \begin{pmatrix} 0 \\ 0 \\ 1 \\ 0 \\ 0 \\ 0 \\ 0 \end{pmatrix}$ and $r_c^3 = \begin{pmatrix} 0 \\ 0 \\ 0 \\ 0 \\ 1 \\ 0 \\ 0 \end{pmatrix}$,

- with $\lambda_{s\pm}$, the eigenvectors are $r_{s\pm} = \begin{pmatrix} \rho^2 \\ \pm\frac{cM_{loc}}{M} \\ 0 \\ c^2 \\ M_{loc}^2\pi + (1-M_{loc}^2)\psi \\ 0 \\ 0 \end{pmatrix}$,

- with $\lambda_{f\pm}$, the eigenvector are $r_{f\pm} = \begin{pmatrix} \rho^2 \\ \pm\frac{c}{MM_{loc}} \\ 0 \\ c^2 \\ M_{loc}^2\pi + (1-M_{loc}^2)\psi \\ \frac{\pm c(1+M_{loc}^2)}{M_{loc}^3 M} \\ \frac{c^2(1+M_{loc}^2)}{M_{loc}^2} \end{pmatrix}$.

After a straightforward computation, we remark that $\nabla_V \lambda \cdot r = 0$ for all pairs (eigenvalue, eigenvector). As a consequence, the system (45) is hyperbolic fully linearly degenerated. Then, the Riemann solution is easily deduced from the Riemann invariants. Indeed, as soon as the j-th field linearly degenerated, the Riemann invariants stay constant across the j-th contact discontinuity. From standard evaluations (see [3,4,7,11]), field by field, the Riemann invariants read as follows:

- associated with λ_c, the Riemann Invariants are

$$\{u, \pi, \psi, \bar{u}\}$$

- associated with $\lambda_{s\pm}$, the Riemann Invariants are

$$\left\{u \pm \frac{cM_{loc}}{\rho M}, \pi \mp \frac{cM}{M_{loc}}u, e - \pi\frac{M_{loc}^2\pi + 2(1-M_{loc}^2)\psi}{2c^2}, v, \psi, \bar{u}\right\}$$

- associated with $\lambda_{f\pm}$, the Riemann Invariants are

$$\left\{\pi + \frac{c^2}{\rho}, \psi - \frac{1+M_{loc}^2}{M_{loc}^2}\pi, \psi \mp c\frac{M(1+M_{loc})^2}{M_{loc}}u, \psi \mp cM_{loc}M\bar{u}, \right.$$
$$\left. e - \frac{M_{loc^2}}{2c^2}(\pi^2 + \frac{1-M_{loc}^2}{1+M_{loc}^2}\psi^2), v\right\}$$

Equipped with these Riemann invariants, their continuity across their associated field yields to a linear system with solution given by (43). The proof is thus completed. □

In the next statement, we establish that the Riemann solution (42)-(43) belongs to Ω_M.

Lemma 4. *For all $M_{loc} < 1$ such that*

$$M \notin \left(\frac{M_{loc}^2}{2 + M_{loc}^2 + \sqrt{1 - M_{loc}^4}}, \frac{M_{loc}^2}{2 + M_{loc}^2 - \sqrt{1 - M_{loc}^4}} \right), \tag{46}$$

there exists $c > 0$ large enough such that the Riemann solution (42)-(43) belongs to Ω_M.

From now on, let us emphasize that the condition (46) must be understood as a restriction to be put on M_{loc}. Here, the Mach number is never restricted. Moreover, in a low Mach number regime, the restriction to be satisfied by M_{loc} is very weak. In addition, we underline that the case $M_{loc} = M$ always satisfies (46).

Proof. The proof is established as soon as both density and internal energy are proved to be positive. Arguing the definition of the intermediate densities, given by (43), we immediately get the required positivity for large enough values of the relaxation parameter c.

In fact, the situation turns out to be more delicate when considering the positiveness of the intermediate internal energy. Here, we solely consider the positiveness of e_{L^*} and e_{C^L} while the establishment of $e_{R^*} > 0$ and $e_{C^R} > 0$ is similar.

Since we are considering large values of c, we suggest to rewrite the intermediate states according to an expansion with respect to c. From the intermediate state definition (43), we get

$$\begin{aligned}
\pi_{L^*} &= c \frac{M_{loc}^3 M}{1 + M_{loc}^2} \frac{(u_L - u_R)}{2} + O(1), \\
\pi_C &= c \frac{M(1 + M_{loc}^2 + M_{loc}^4) - M_{loc}^2}{M_{loc}(1 + M_{loc}^2)} \frac{(u_L - u_R)}{2} + O(1), \\
\psi_C &= c M M_{loc} \frac{(u_L - u_R)}{2} + O(1).
\end{aligned}$$

For the sake of clarity in the notations, we set

$$\begin{aligned}
\theta_1 &= \frac{M_{loc}^3 M}{1 + M_{loc}^2}, \\
\theta_2 &= \frac{M(1 + M_{loc}^2 + M_{loc}^4) - M_{loc}^2}{M_{loc}(1 + M_{loc}^2)},
\end{aligned} \tag{47}$$

in order to write

$$\begin{aligned}
\pi_{L^*} &= c\theta_1 \frac{(u_L - u_R)}{2} + O(1), \\
\pi_C &= c\theta_2 \frac{(u_L - u_R)}{2} + O(1).
\end{aligned}$$

According to the definition of e_{L^*}, given by (43), we obtain

$$e_{L^*} = e_L + M_{loc}^2 \left(\theta_1^2 + \frac{1 - M_{loc}^2}{1 + M_{loc}^2} \theta_2^2 \right) \frac{(u_L - u_R)^2}{8} + O\left(\frac{1}{c}\right)$$

With $M_{loc} \in (0,1)$, since $e_L > 0$, we get $e_{L^*} > 0$ as soon as c is large enough.

Now, the expansion of e_{C^L} with respect to c reads as follows:

$$e_{C^L} = e_L + f(M_{loc}, M) \frac{(u_L - u_R)^2}{8} + O\left(\frac{1}{c}\right)$$

where we have set

$$f(M_{loc}, M) = \left(M_{loc}^2 \frac{1 - M_{loc}^2}{1 + M_{loc}^2} M^2 M_{loc}^2 + M_{loc}^2 \theta_2^2 - 2(1 - M_{loc}^2) M M_{loc} (\theta_1 - \theta_2) \right).$$

The quantity e_{C^L} will be proved to be positive as soon as $f(M_{loc}, M)$ is fixed non-negative. By definition of θ_1 and θ_2, given by (47), we write

$$f(M_{loc}, M) = \frac{(3 + 4M_{loc}^2 + 2M_{loc}^4) M^2 - M(4M_{loc}^2 + 2M_{loc}^4) + M_{loc}^4}{(1 + M_{loc}^2)^2}.$$

Since the denominator is always positive we only have to consider the numerator as given in the following function:

$$\mathcal{N}(M_{loc}, M) = (3 + 4M_{loc}^2 + 2M_{loc}^4) M^2 - M(4M_{loc}^2 + 2M_{loc}^4) + M_{loc}^4$$

The function $\mathcal{N}$ is a quadratic convex function with respect to M and it admits the following roots:

$$M_{\pm} = \frac{M_{loc}^2}{2 + M_{loc}^2 \pm \sqrt{1 - M_{loc}^4}}. \tag{48}$$

The required non-negativity of the function $f(M_{loc}, M)$ is thus satisfied as long as M does not belong to (M_+, M_-). The proof is achieved. □

To conclude the presentation of the main properties satisfied by the Riemann solutions of system $(35)_{\varepsilon=\infty}$, we now show that such solutions coincide, in a sense to be prescribed, with the Riemann solutions of system $(20)_{\varepsilon=\infty}$ in the limit of M_{loc} to 1. As a consequence, the all Mach number relaxation scheme (17)-(18)-(44) may coincide with the standard Suliciu relaxation scheme (17)-(18)-(24) which performs well when the flow is not in the low Mach number regime.

Lemma 5. *In the limit of M_{loc} to 1, the vector*

$$\tilde{U}_{\mathcal{R}}(\frac{x}{t}; W_L, W_R) = {}^t(\rho, \rho u, \rho v, E, \rho\pi),$$

extracted from the Riemann solution (42)-(43) of $(35)_{\varepsilon=\infty}$ tends to the vector $U_{\mathcal{R}}(\frac{x}{t}, U_L, U_R)$, defined by (22)-(23), solution of the Riemann problem associated with $(20)_{\varepsilon=\infty}$.

Proof. When M_{loc} tends to 1, the last two equations in $(35)_{\varepsilon=\infty}$ do not have any influence one the rest of the system. As a consequence, the extracted system from $(35)_{\varepsilon=\infty}$ to govern ${}^t(\rho, \rho u, \rho v, E, \rho\pi)$ is identical to the standard relaxation system $(20)_{\varepsilon=\infty}$. □

3.3 Low Mach number properties of the new relaxation scheme

In this section, we study the properties satisfied by the derived all Mach number relaxation scheme. In fact, we are here interested in two properties. The first one concerns the behavior of the numerical diffusion. Indeed, after (31), the numerical viscosity may become preponderant as M goes to zero by producing very large numerical error. We will show that such a failure is corrected by adopting the numerical scheme (17)-(18)-(44). The second property of main interest is the so-called Asymptotic-Preserving property. Indeed, in the limit of M to zero, we will establish that the scheme converges to a consistent discretization of the expected incompressible model flow.

Within this asymptotic analysis, we adopt $M_{loc} = M$ since such a choice is relevant and satisfies the restriction (46).

First, let us exhibit the behavior of the numerical diffusion given by

$$D(w_R - w_L) = \frac{1}{2}\left(f(w_L) + f(w_R)\right) - f(w_L, w_R), \tag{49}$$

where D stands for the numerical diffusion matrix and $f(w_L, w_R)$ is the numerical flux function defined by (18)-(44). In a first step, we adopt the rescaling (25) supplemented by the scaling of the new relaxation variables as follows:

$$\begin{aligned} &\psi_L = p_0 + O(M^2), && \psi_R = p_0 + O(M^2),\\ &\bar{u}_L = u_{0,L} + O(M), && \bar{u}_R = u_{0,R} + O(M). \end{aligned}$$

Arguing the definition of the intermediate states, given by (43), the following scaling of the intermediate states directly holds:

$$\begin{aligned} &u_{L^*} = u_{0,L} + O(M), && u_{R^*} = u_{0,R} + O(M), && (50)\\ &\rho_{L^*} = \rho_0 + O(M), && \rho_{R^*} = \rho_0 + O(M), && (51)\\ &\rho_{C^L} = \rho_0 + O(1), && \rho_{C^R} = \rho_0 + O(1), && (52)\\ &\pi_C = p_0 + O(1), && u_C = u_{0,L/R} + O(1), && (53)\\ &\pi_{L^*} = p_0 + O(M^2), && \pi_{R^*} = p_0 + O(M^2), && (54)\\ &\psi_C = p_0 + O(M^2), && \bar{u} = u_{0,L/R} + O(1), && (55)\\ &e_{L^*} = e_{0,L} + O(M), && e_{R^*} = e_{0,R} + O(M), && (56)\\ &e_{C^L} = e_{0,L} + O(1), && e_{C^R} = e_{0,R} + O(1), && (57)\\ &v_{L^*} = v_{C^L} = v_{0,L} + O(M), && v_{R^*} = v_{C^R} = v_{0,R} + O(M). && (58) \end{aligned}$$

A straightforward computation yields to the following asymptotic behavior satisfied by the numerical flux function:

$$f(w_L, w_R) = \begin{pmatrix} \rho_0 u_{0,L/R} + O(1) \\ \rho_0 u_{0,L/R}^2 + \frac{p_0}{M^2} + O(1) \\ \rho_0 u_{0,L/R} v_{0,L/R} + O(1) \\ (u_{0,L/R}(E_0 + p_0)) + O(1) \end{pmatrix}$$

Therefore, the behavior of the diffusion is given by

$$D = \begin{pmatrix} O(1) \\ O(1) \\ O(1) \\ O(1) \end{pmatrix}. \tag{59}$$

As a consequence, the numerical viscosity of the derived numerical scheme (17)-(18)-(44) does not depend on the Mach number. Put in other words, as M goes to zero, the numerical error does not dominate the simulation at the discrepancy with the standard Suliciu relaxation scheme (17)-(18)-(24).

Next, we turn considering some AP-properties satisfied by the derived scheme. More precisely, in the limit of M to zero, we have to recover the asymptotic regime governed by (9)-(10). To address such an issue, we have to consider the full 2D-scheme as defined in (17)-(18)-(44). Once again, we assume the same scaling for M and M_{loc} and thus we enforce $M_{loc} = M$.

First, we consider the discrete equation for the x-momentum given by

$$(\rho u)_{i,j}^{n+1} = (\rho u)_{i,j}^{n} - \frac{\Delta t}{\Delta x}\left(f_{i+1/2,j}^{\rho u,n+1} - f_{i-1/2,j}^{\rho u,n+1} + g_{i,j+1/2}^{\rho u,n+1} - g_{i,j-1/2}^{\rho u,n+1}\right), \tag{60}$$

where, with clear notations to define the numerical flux function at the interface $x_{i+1/2}$, we have set

$$\begin{aligned} f_{i\pm1/2,j}^{\rho u,n+1} &= (\rho u^2)_{i\pm1/2,j}^{n+1} + \pi_{i\pm1/2,j}^{n+1} + \frac{1-M^2}{M^2}\psi_{i\pm1/2,j}^{n+1}, \\ g_{i,j\pm1/2}^{\rho u,n+1} &= (\rho uv)_{i,j\pm1/2}^{n+1}. \end{aligned}$$

Next, we multiply (60) with M^2 to get

$$\begin{aligned} M^2\left((\rho u)_{i,j}^{n+1} - (\rho u)_{i,j}^{n}\right) = &-(1-M^2)\frac{\Delta t}{\Delta x}\left(\psi_{i+1/2,j}^{n+1} - \psi_{i-1/2,j}^{n+1}\right) - \\ &M^2\frac{\Delta t}{\Delta x}\left((\rho u^2)_{i+1/2,j}^{n+1} + \pi_{i+1/2,j}^{n+1} - (\rho u^2)_{i-1/2,j}^{n+1} - \right. \\ &\left.\pi_{i-1/2,j}^{n+1} + (\rho uv)_{i,j+1/2}^{n+1} - (\rho uv)_{i,j-1/2}^{n+1}\right) \end{aligned}$$

Let us assume that both discrete time derivative and numerical flux function are bounded in M. Therefore, as M goes to 0, we get

$$0 = \psi_{i+1/2,j}^{n+1} - \psi_{i-1/2,j}^{n+1}.$$

With the definition of ψ we also have

$$\lim_{M\to 0} \psi^{n+1}_{i+1/2,j} = \frac{p^{n+1}_{i+1,j} + p^{n+1}_{i,j}}{2}.$$

Therefore we obtain

$$p^{n+1}_{i+1,j} = p^{n+1}_{i-1,j}. \tag{61}$$

By symmetry, from the equation for the y-momentum, we also have

$$p^{n+1}_{i,j+1} = p^{n+1}_{i,j-1}. \tag{62}$$

Equipped with these computations, we are now able to state the following result.

Lemma 6. *Consider the scheme (17)-(18)-(44) and denote by N_x and N_y the number of grid points in the x and y direction respectively. Further assume that the pressure at the boundary is determined by*

$$\forall_{j\in[1,N_y]} \quad p^{n+1}_{0,j} = p^{n+1}_{N_x+1,j} = p_0 \quad \textit{and} \quad \forall_{i\in[1,N_x]} \quad p^{n+1}_{i,0} = p^{n+1}_{i,N_y+1} = p_0. \tag{63}$$

Then, if at least one of N_x and N_y is even, there is

$$\forall_{i,j} = p^{n+1}_{i,j} = p_0 \tag{64}$$

Proof. Consider the case that N_x is even. From (61), there is for any j and any integer $k \in \{1, N_x/2\}$

$$p^{n+1}_{0,j} = p^{n+1}_{2k,j} = p_0. \tag{65}$$

Conversely we have

$$p^{n+1}_{N_x+1,j} = p^{n+1}_{2k-1,j} = p_0. \tag{66}$$

Since j was arbitrary and the same argument holds if N_y is even, this concludes the proof. □

Next we consider the energy equation given by

$$E^{n+1}_{i,j} = E^n_{i,j} - \frac{\Delta t}{\Delta x}\left(f^E_{i+1/2,j} - f^E_{i-1/2,j} + g^E_{i,j+1/2} - g^E_{i,j-1/2}\right), \tag{67}$$

where we have set

$$f^E_{i+1/2,j} = (u(E + M^2\pi + (1-M^2)\psi))_{i+1/2,j},$$
$$g^E_{i,j+1/2} = (v(E + M^2\pi + (1-M^2)\psi))_{i,j+1/2}.$$

Because of (3), we have the following limit:

$$\lim_{M\to 0} E = \rho e = \frac{p}{\gamma - 1}. \tag{68}$$

Then, from (64) and (68), we obtain

$$\lim_{M\to 0}\left(E_{i,j}^{n+1}-E_{i,j}^{n}\right)=\frac{p_0}{\gamma-1}-\frac{p_0}{\gamma-1}=0. \tag{69}$$

Next, consider the numerical fluxes in the x-derivative. In the limit of M to 0, we get

$$f_{i+1/2,j}^{E,0}:=\lim_{M\to 0} f_{i+1/2,j}^{E}=(u((\rho e)+\psi))_{i+1/2,j}. \tag{70}$$

From (64) and by definition of $\psi_{i+1/2,j}$ given by (43), we have

$$\lim_{M\to 0}\psi_{i+1/2,j}=p_0. \tag{71}$$

Moreover, in the low Mach number limit, the numerical flux function is defined by the intermediate states $C^{L,R}$ given by (43). As a consequence, we obtain

$$\begin{aligned}
&\lim_{M\to 0} u_{i+1/2,j}=\frac{u_{0,i,j}+u_{0,i+1,j}}{2},\\
&\lim_{M\to 0}\rho_{i+1/2,j}=(\rho_0+\frac{\rho_0^2(u_{0,i,j}-u_{0,i+1,j})}{2c+\rho_0(u_{0,i+1,j}-u_{0,i,j})}),\\
&\lim_{M\to 0} e_{i+1/2,j}=(e_{0,i/i+1,j}+p_0\frac{u_{0,i,j}-u_{0,i+1,j}}{2c}).
\end{aligned}$$

Since, we reject the possibility of shocks in the low Mach number limit, therefore we have

$$u_{0,i,j}-u_{0,i+1,j}=\Delta_{u,i+\frac{1}{2},j}=O(\Delta x). \tag{72}$$

After performing a expansion of $\rho_{i+1/2,j}$ in $\Delta_{u,i+\frac{1}{2},j}$, up to second-order terms, we write the numerical flux as follow:

$$\begin{aligned}
f_{i+1/2,j}^{E,0}&=\frac{u_{0,i,j}+u_{0,i+1,j}}{2}\left(\frac{\gamma}{\gamma-1}p_0+\Delta_{u,i+\frac{1}{2},j}\frac{\rho_0}{2c}p_0\right)+O(\Delta x^2),\\
&=\frac{u_{0,i,j}+u_{0,i+1,j}}{2}\frac{\gamma}{\gamma-1}p_0-\frac{u_{0,i+1,j}^2-u_{0,i,j}^2}{2}\frac{\rho_0}{2c}p_0+O(\Delta x^2).
\end{aligned}$$

Then we immediately get

$$\begin{aligned}
&f_{i+1/2,j}^{E,0}-f_{i-1/2,j}^{E,0}=\\
&\frac{u_{0,i+1,j}-u_{0,i-1,j}}{2}\frac{\gamma}{\gamma-1}p_0-\frac{u_{0,i+1,j}^2-2u_{0,i}^2+u_{0,i+1,j}^2}{2}\frac{\rho_0}{2c}p_0+O(\Delta x^2).
\end{aligned} \tag{73}$$

Since the analysis in the y-direction is analogous, from (69) and (73), we simplify (67) as follows:

$$\begin{aligned}
0=&-\frac{1}{\Delta x}(\frac{u_{0,i+1,j}-u_{0,i-1,j}}{2}\frac{\gamma}{\gamma-1}p_0-\frac{u_{0,i+1,j}^2-2u_{0,i,j}^2+u_{0,i-1,j}^2}{2}\frac{\rho_0}{2c}p_0)\\
&-\frac{1}{\Delta x}(\frac{v_{0,i,j+1}-v_{0,i,j-1}}{2}\frac{\gamma}{\gamma-1}p_0-\frac{v_{0,i,j+1}^2-2v_{0,i,j}^2+v_{0,i,j-1}^2}{2}\frac{\rho_0}{2c}p_0)+O(\Delta x).
\end{aligned}$$

According to suitable assumptions on the regularity (72) of the dependent variables, we write

$$0 = -\left(u(x_i,y_j)_x + v(x_i,y_j)_y\right) + \Delta x \left(u(x_i,y_j)_{x,x}^2 + v(x_i,y_j)_{y,y}^2\right) \frac{\gamma-1}{\gamma}\frac{\rho_0}{2c} + O(\Delta x).$$

Therefore, in the low Mach number limit, the energy equation (67) reduces as follows:

$$div(u,v) = \Delta x \Delta(u^2,v^2)\frac{\gamma-1}{\gamma}\frac{\rho_0}{2c} + O(\Delta x), \tag{74}$$

and gives the divergence constraint for the velocity field with a diffusion term that vanishes in the limit of Δx to 0. Summing the previous derivations we can state the following result.

Theorem 7. *The numerical scheme defined by (17)-(18)-(44), under the assumptions of Lemma 6, is asymptotic preserving when M tends to* 0.

4 Numerical results

Now, the proposed low Mach number scheme is tested for its practical applicability. In all test cases, an ideal gas law is used with $\gamma = \frac{5}{3}$ as well as an equidistant grid. The emphasis in these tests lies in the comparison of the new relaxation scheme with respect to the standard Suliciu relaxation scheme. By comparison between (23) and (43), it is clear that the standard scheme is recovered when choosing $M_{loc} = 1$. The new relaxation scheme is denoted as S_M while S_1 denotes the standard relaxation scheme.

4.1 SOD Shock Tube test

The first test case investigates the capability of the low Mach number scheme to deal with discontinuities. To this end, the Sod shock tube test is concerned, see [26]. The computational domain is $D = [0,1]$ and the initial conditions are set as

$$(\rho(0,x),u(0,x),p(0,x)) = \begin{cases} (1.0,0,1.0) & \text{if} \quad x < 0.5, \\ (0.125,0,0.1) & \text{if} \quad x > 0.5. \end{cases} \tag{75}$$

Only first order versions of the scheme S_M are concerned in order to investigate the influence of the numerical flux function on the approximation. Moreover, in this test case an explicit time integration is performed. In order to perform an explicit time integration the local Mach number has to be controlled in order for the fastest eigenvalues in (41) to be bounded. Therefore in this case we set $M = M_{loc}$ that also satisfies (46). The results are shown in figure 3.

When looking at the numerical approximations with 100 cells and comparing them with the solutions on higher resolutions, a similar behaviour on all the different Mach numbers can be observed. At first, the low Mach number scheme

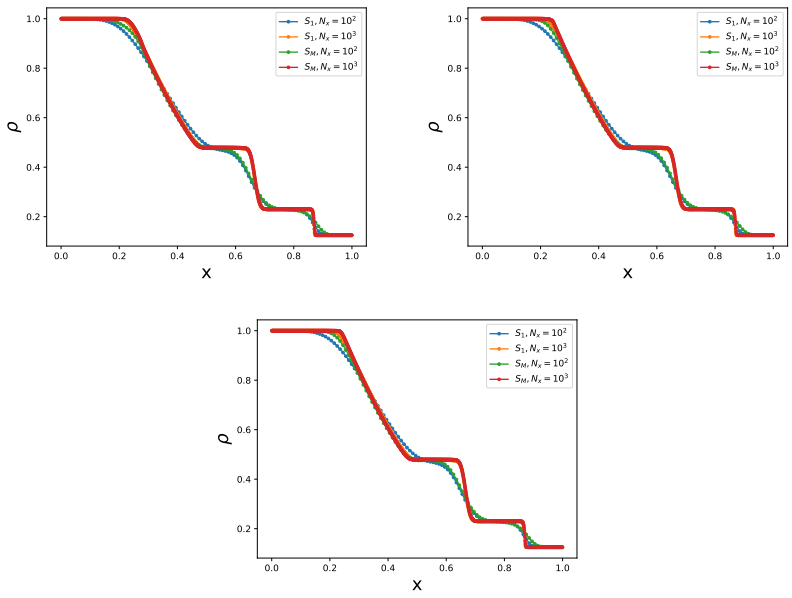

Figure 3: Numerical approximations to the SOD shock tube test for the schemes S_1 and S_M at different Mach numbers and at different resolutions at time 0.2. Top left: $M = 10^{-1}$. Top right: $M = 10^{-2}$. Bottom center: $M = 10^{-3}$.

seems to be more diffusive on the shock around 0.9. Both schemes show a comparable performance on the contact discontinuity at 0.6, while the rarefaction wave is much better captured by the low Mach number scheme. Moreover, both schemes are in good agreement in all regimes when the resolution is increased.

4.2 Gresho Vortex test

A classical test case for low Mach number properties is the Gresho vortex. The Gresho vortex is an axisymmetric steady state solution of the compressible Euler equations and the velocity field satisfies the free divergence condition from the incompressible limit. Here the modified version from [18] is considered. It is defined in polar coordinates and by axisymmetry only the radial component needs to be specified. Denoting by u_ϕ the angular velocity, it is set as

$$u_\phi(r) = \begin{cases} 5r & \text{if} \quad 0 \le r \le 0.2, \\ 2 - 5r & \text{if} \quad 0.2 \le r \le 0.4, \\ 0 & \text{if} \quad 0.4 \le r, \end{cases} \tag{76}$$

and the pressure distribution is given by

$$p(r) = p_0 + \begin{cases} \frac{25}{2} r^2 & \text{if} \quad 0 \le r \le 0.2, \\ \frac{25}{2} r^2 + 4(1 - 5r - \ln 0.2 + \ln r) & \text{if} \quad 0.2 \le r \le 0.4, \\ 4 \ln 2 - 2 & \text{if} \quad 0.4 \le r, \end{cases} \tag{77}$$

where $p_0 = \frac{\rho}{\gamma M^2}$. The density ρ is considered as constant and the computational domain is $D = [-1, 1] \times [-1, 1]$. Fixing ρ, the reference Mach number M is used to scale the vortex to different regimes. The respective schemes are implemented in the SLH code [17], where the implicit time integration method ESDIRK34 from [15] is used. In order to ensure a suitable convergence behavior for the Newton iteration the slopes are not limited, but are chosen as differentiable functions from the cell centered values from neighboring cells, see also [17]. In order to see how the schemes perform on a low resolution the simulations are performed on an equidistant grid in both spatial dimensions with $N_x = N_y = 40$ and periodic boundary conditions are imposed. The resulting distributions of the relative Mach number, i.e. $M_{rel}(t, x, y) = \frac{M_{loc}(t,x,y)}{M}$, after one rotation for different reference Mach numbers are shown in figure 4.

The scheme S_1 introduces an increasing amount of diffusion with decreasing Mach number; as can be seen in the top row of figure 4. In contrast to that, the new relaxation scheme S_M preserves the vortex structure on all Mach numbers equally good. This result is expected form the derivations of the numerical diffusion of the upwind schemes S_1 in (31) and S_M in (59).

Another criterion to check the quality of the numerical approximation is the kinetic energy. Since the vortex is a stationary solution, the kinetic energy also remains constant in the exact solution. The evolution of the total kinetic energy in the computational domain is shown in figure 5.

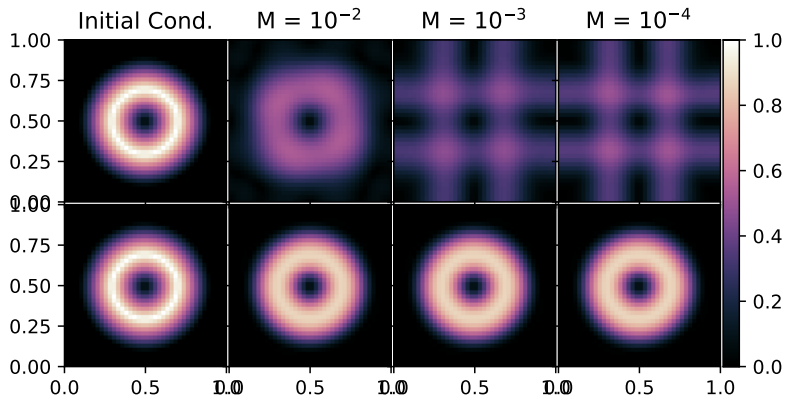

Figure 4: Local relative Mach number for the Gresho Vortex after one rotation at different Mach numbers. Top: results for the scheme S_1. Bottom: results for the scheme S_M.

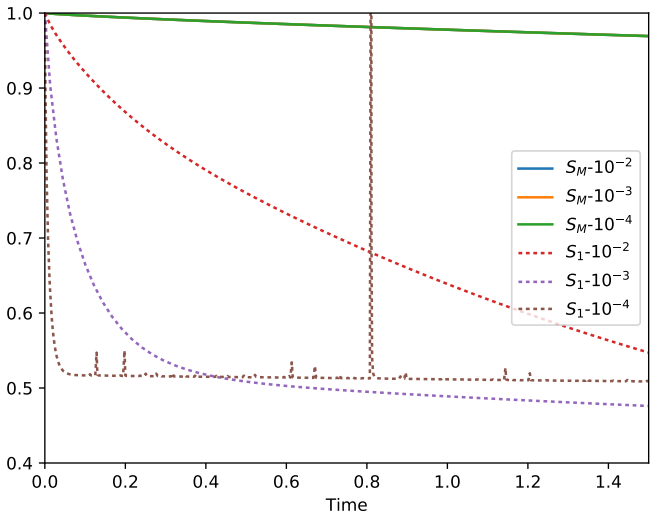

Figure 5: Evolution of the total kinetic energies in the numerical approximation of the Gresho vortex at different Mach numbers for different schemes. Shown is the relative total kinetic energy, i.e. $\frac{tKE(t)}{tKE(0)}$.

The scheme S_1 shows an increasing diffusion of the kinetic energy by decreasing Mach number. Even more, for Mach number 10^{-4}, the scheme actually shows also convergence problems and the solution becomes unphysical. On the other hand the scheme S_M shows only a small diffusion of the kinetic energy and the diffusion of the total relative kinetic energy is practically identical at the different Mach numbers.

4.3 Kelvin Helmholtz Instability

The last test case concerns the approximation of a Kelvin-Helmholtz instability. The idea is to introduce a non steady flow problem to further investigate the influence of the numerical diffusion on the quality of the numerical approximations. The setup is also taken from [18], where the shear instability is triggered artificially to enforce a specific behavior of the resulting vortices. This gives the possibility to compare the results for different schemes. Therefore the initial conditions are set as

$$\rho = \begin{cases} \rho_1 - \rho_m \exp(\frac{y-0.25}{L}) & \text{if} \quad 0 \leq y \leq 0.25, \\ \rho_2 + \rho_m \exp(\frac{-y+0.25}{L}) & \text{if} \quad 0.25 \leq y \leq 0.5, \\ \rho_2 + \rho_m \exp(\frac{y-0.75}{L}) & \text{if} \quad 0.5 \leq y \leq 0.75, \\ \rho_1 - \rho_m \exp(\frac{-y+0.75}{L}) & \text{if} \quad 0.75 \leq y \leq 1, \end{cases}$$

and

$$u = \begin{cases} u_1 - u_m \exp(\frac{y-0.25}{L}) & \text{if} \quad 0 \leq y \leq 0.25, \\ u_2 + u_m \exp(\frac{-y+0.25}{L}) & \text{if} \quad 0.25 \leq y \leq 0.5, \\ u_2 + u_m \exp(\frac{y-0.75}{L}) & \text{if} \quad 0.5 \leq y \leq 0.75, \\ u_1 - u_m \exp(\frac{-y+0.75}{L}) & \text{if} \quad 0.75 \leq y \leq 1, \end{cases}$$

and $p = 2.5$. The parameters are

$$\rho_1 = 1.0 \qquad \rho_2 = 2.0 \qquad \rho_m = \frac{\rho_1 - \rho_2}{2},$$
$$u_1 = 1.0 \qquad u_2 = 2.0 \qquad u_m = \frac{\rho_1 - \rho_2}{2},$$

and $L = 0.025$. The computational domain is $D = [0, 1] \times [0, 1]$ and periodic boundary conditions are imposed. The instability is triggered by a perturbation in the vertical velocity as

$$v = 10^{-2} \sin(2\pi x)$$

and the simulations are performed with a Mach number of $M = 10^{-2}$. The results are depicted in figure 6 and figure 7.

From figure 7 we have that the flow regime is in the regime of a Mach number $M \approx 10^{-4}$. From the Gresho vortex test we therefore expect a significant improvement by the introduction of the new relaxation scheme S_M. The superior

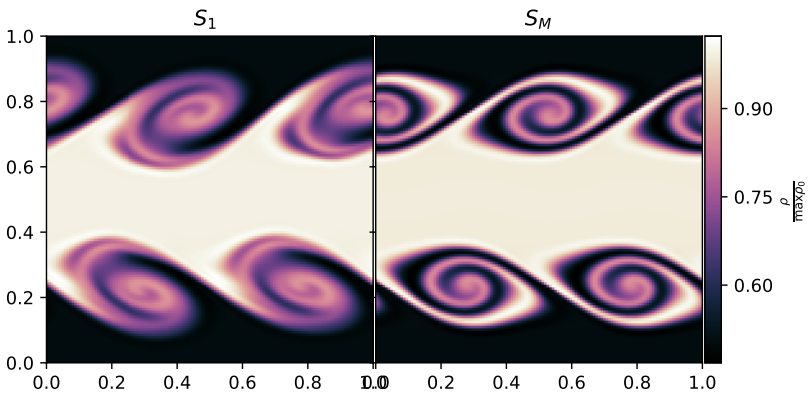

Figure 6: Kelvin-Helmholtz Instability computed with the schemes S_1 and S_M on a 128×128 grid.

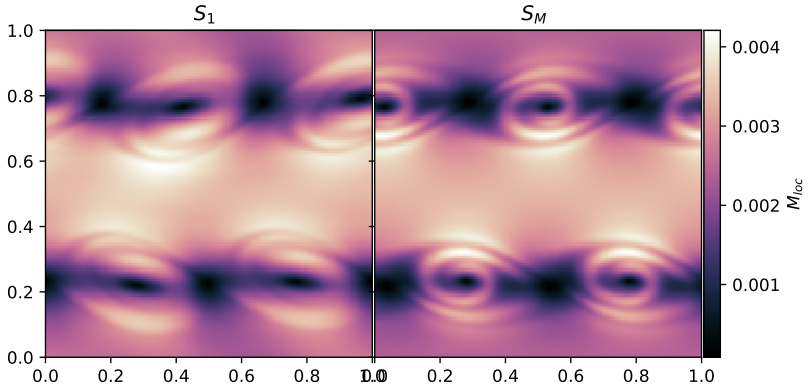

Figure 7: Kelvin-Helmholtz Instability computed with the schemes S_1 and S_M on a 128×128 grid.

performance can be seen in figure 6. The resulting vortices are better resolved by the scheme S_M then with the scheme S_1.

5 Conclusion

In this work we are concerned with the low Mach number approximation of flows governed by the compressible Euler equations. We have used the standard Suliciu relaxation technique and showed, that it is not useful for the approximation of these flow regimes. Then we construct a modified relaxation scheme and show, that the numerical diffusion of the upwind scheme is controlled in the low Mach number case, that the relaxation scheme is robust with respect to the positivity of density and internal energy and show the asymptotic preserving property of the new scheme. We then give numerical tests to show the superior performance of the modified relaxation scheme compared to a standard scheme.

6 Acknowledgments

We thank DAAD Procope and also the Bayerische Französische Hochschulzentrum for partially supporting this work.

References

[1] Guillard H. & Murrone A. On the behavior of upwind schemes in the low mach number limit: II. godunov type schemes. *Computers & Fluids*, 33:655–675, 2004.

[2] Klainerman S. & Majda A. Singular limits of quasilinear hyperbolic systems with large parameters and the incompressible limit of compressible fluids. *Communications on Pure and Applied Mathematics*, 34(4):481–524, July 1981.

[3] Coquel F. & Pertham B. Relaxation of energy and approximate riemann solvers for general pressure laws in fluid dynamics. *SIAM Journal on Numerical Analysis*, 35(6):2223–2249, 1998.

[4] M. Baudin, C. Berthon, F. Coquel, R. Masson, and Q. H. Tran. A relaxation method for two-phase flow models with hydrodynamic closure law. *Numerische Mathematik*, 99(3):411–440, 2005.

[5] Guillard H. & Viozat C. On the behaviour of upwind schemes in the low mach number limit. *Computers & Fluids*, 28:63–86, 1999.

[6] Noelle S. & Bispen G. & Arun K.R. & Lukáčová-Medvid´ová & Munz C.D. An asymptotic preserving all mach number scheme for the euler equations of gas dynamics. *SIAM Journal of Scientific Computing*, 36(6):989–1024, 2014.

[7] C. Chalons, F. Coquel, E. Godlewski, P.-A. Raviart, and N. Seguin. Godunov-type schemes for hyperbolic systems with parameter-dependent source. The case of Euler system with friction. *Math. Models Methods Appl. Sci.*, 20(11):2109–2166, 2010.

[8] Turkel E. Preconditioned methods for solving the incompressible and low speed compressible equations. *Journal of Computational Physics*, 72, 1987.

[9] Barsukow W. & Edelmann P. & Klingenberg C. & Miczek F& Röpke F. A numerical scheme for the compressible low-mach number regime of idela fluid dynamics. *Journal of Scientific Computing*, 72(2):623–646, 2017.

[10] Bouchut F. *Nonlinear Stability of Finite Volume Methods for Hyperbolic Conservation Laws and Well-Balanced Schemes for Sources.* Birkhäuser Verlag, 2004.

[11] E. Godlewski and P.-A. Raviart. *Numerical approximation of hyperbolic systems of conservation laws*, volume 118 of *Applied Mathematical Sciences.* Springer-Verlag, New York, 1996.

[12] A. Harten, P.D. Lax, and B. Van Leer. On upstream differencing and Godunov-type schemes for hyperbolic conservation laws. *SIAM review*, 25:35–61, 1983.

[13] Suliciu I. On modelling phase transitions by means of rate-type constitutive equations, shock wave structure. *International Journal of Engineering Science*, 28:829–841, 1990.

[14] Haack J. & Jin S. & Liu J. An all-speed asymptotic-preserving method for the isentropic euler and navier-stokes equations. *Communications in Computational Physics*, 12(4):955–980, 2012.

[15] C. A. Kennedy and M. H. Carpenter. Additive runge-kutta schemes for convection-diffusion-reaction equation. *Tech. rep., NASA Technical Memorandum*, 2001.

[16] Degond P. & Tang M. All speed scheme for the low mach number limit of the isentropic euler equations. *Communications in Computational Physics*, 10(1):1–31, 2011.

[17] F. Miczek. *Simulation of low Mach number astrophysical flows*. PhD thesis, München, Technische Universität München, Diss., 2013.

[18] F. Miczek, Röpke F. K., and Edelmann P. V. F. A new numerical solver for flows at various mach numbers. *Astronomy and Astrophysics*, 576(A50):16, April 2015.

[19] B. Perthame and C. W. Shu. On positivity preserving finite volume schemes for Euler equations. *Numerische Mathematik*, 73(1):119–130, 1996.

[20] Roe P.L. Approximate riemann solvers, parameter vectors, and difference schemes. *Journal of Computational Physics*, 43(2):357–372, 1981.

[21] Klein R. Semi-implicit extension of a godunov-type scheme based on low mach number asymptotics i: One-dimensional flow. *Journal of Computational Physics*, 121(2):213–237, October 1995.

[22] Bispen G. & Arun K.R. & Lukáčová-Medvid´ová M. & Noelle S. IMEX large time step finite volume methods for low froude number shallow water flows. *Communications in Computational Physics*, 16(2):307–347, August 2014.

[23] Dellacherie S. Analysis of godunov type schemes applied to the compressible euler system at low mach number. *Journal of Computational Physics*, 229(4):978–1016, February 2010.

[24] Feireisl E. & Klingenberg C. & Markfelder S. On the low mach number limit for the compressible euler system. *preprint, https://arxiv.org/abs/1804.09509*.

[25] Jin S. Efficient asymptotic-preserving (ap) schemes for some multiscale kinetic equations. *SIAM Journal of Scientific Computing*, 21(2):441–454, 1999.

[26] Gary A Sod. A survey of several finite difference methods for systems of nonlinear hyperbolic conservation laws. *Journal of Computational Physics*, 27(1):1 – 31, 1978.

[27] I. Suliciu. Some stability-instability problems in phase transitions modelled by piecewise linear elastic or viscoelastic constitutive equations. *International Journal of Engineering Science*, 30:483–494, 1992.

[28] R. Klein & Botta N. & Schneider T. & Munz C.D. & Roller S. & Meister A.& Hoffmann L. & Sonar T. Asymptotic adaptive methods for multi-scale problems in fluid mechanics. *Journal of Engineering Mathematics*, 39(1):261–343, 2001.

[29] Chen G.Q. & Levermore C.D. & Liu T.-P. Hyperbolic conservation laws with stiff relaxation terms and entropy. *Communications on Pure and Applied Mathematics*, 47:787–830, 1994.

[30] J.M. Weiss and W.A. Smith. Preconditioning applied to variable and constant density flows. *AIAA Journal*, 33(11):2050–2057, 1995.

[31] G. B. Whitham. *Linear and nonlinear waves*. Wiley-Interscience [John Wiley & Sons], New York-London-Sydney, 1974. Pure and Applied Mathematics.